

# Analytical Methods

Accepted Manuscript



This is an *Accepted Manuscript*, which has been through the Royal Society of Chemistry peer review process and has been accepted for publication.

*Accepted Manuscripts* are published online shortly after acceptance, before technical editing, formatting and proof reading. Using this free service, authors can make their results available to the community, in citable form, before we publish the edited article. We will replace this *Accepted Manuscript* with the edited and formatted *Advance Article* as soon as it is available.

You can find more information about *Accepted Manuscripts* in the [Information for Authors](#).

Please note that technical editing may introduce minor changes to the text and/or graphics, which may alter content. The journal's standard [Terms & Conditions](#) and the [Ethical guidelines](#) still apply. In no event shall the Royal Society of Chemistry be held responsible for any errors or omissions in this *Accepted Manuscript* or any consequences arising from the use of any information it contains.

1  
2  
3 **Homogeneous surface-enhanced Raman scattering platform for ultra-trace**  
4 **detection of trinitrotoluene in environment**  
5  
6  
7  
8  
9

10  
11 Arniza K. M. Jamil<sup>a</sup>, Emad L. Izake<sup>a\*</sup>, Arumugam Sivanesan<sup>a\*</sup>, Roland Agoston<sup>a</sup>, Godwin A.  
12  
13 Ayoko<sup>a</sup>  
14  
15

16  
17 <sup>a</sup> Nanotechnology and Molecular Sciences Discipline, Faculty of Science and Engineering,  
18  
19 Queensland University of Technology, 2 George St., Brisbane, QLD 4001, Australia.  
20  
21

22  
23  
24 A.S. and A.K.M.J contributed equally to the manuscript  
25  
26

27  
28 \*Corresponding authors:  
29

30  
31  
32 E-mail address: [sivanesan.arumugam@qut.edu.au](mailto:sivanesan.arumugam@qut.edu.au); [asnesan@gmail.com](mailto:asnesan@gmail.com) (A. Sivanesan) Tel: +61 07  
33  
34 3138 0607  
35

36  
37 E-mail address: [e.kiriakous@qut.edu.au](mailto:e.kiriakous@qut.edu.au) (E. L. Izake) Tel.: +61 7 3138 2501; Fax: +61 7 3138 1804  
38  
39  
40  
41  
42  
43  
44  
45  
46  
47  
48  
49  
50  
51  
52  
53  
54  
55  
56  
57  
58  
59  
60

## Abstract

A facile and sensitive surface-enhanced Raman scattering substrate was prepared by controlled potentiostatic deposition of closely packed single layer of gold nanostructures (AuNS) over flat gold (pAu) platform. The nanometer scale inter-particle distance between the particles resulted in high population of 'hot spot' which enormously enhanced the scattered Raman photons. A renewed methodology was followed to precisely quantify the SERS substrate enhancement factor (SSEF) and it was estimated as  $(2.2 \pm 0.17) \times 10^5$ . The reproducibility of the SERS signal acquired by the developed substrate was tested by establishing the relative standard deviation (RSD) of 150 repeated measurements from various locations on the substrate surface. A low RSD of 4.37 confirmed the homogeneity of the developed substrate. The sensitivity of pAu/AuNS was proven by determining 100 fM 2,4,6-trinitrotoluene (TNT) comfortably. As a proof of concept on the potential of the new pAu/AuNS substrate in field analysis, TNT in soil and water matrices was selectively detected after forming a Meisenheimer complex with cysteamine.

**Keywords:** Reproducible surface-enhanced Raman nanosensor; ultra-sensitive and homogeneous nanostructure assembly; 2,4,6-trinitrotoluene (TNT); soil and water analyses

## 1. Introduction

In recent years, surface-enhanced Raman spectroscopy (SERS) has become a very sensitive analytical technique for identifying traces of analytes ranging from small chemicals to macromolecules/microorganisms such as bacteria and viruses.<sup>1-6</sup> Nevertheless, the sensitivity of SERS technique largely relies on the presence of a sensitive substrate i.e., a strong enhancing surface for the incident” and Raman photons by plasmon resonance.<sup>7-9</sup> SERS enhancement is a joint effect of electromagnetic and chemical enhancement, the former is a predominant contributor to the observed enhancement, in particular on metallic surfaces.<sup>7, 8</sup> Ultimately, a surface plasmon rich metallic surface is the prime requirement for large SERS enhancement. Noble metal nanoparticles represent the best candidate to vastly amplify the scattered Raman photons since they have a strong plasmon cloud extending up to several nanometers away from the surface.<sup>10, 11</sup> Numerous literature have been published in the past decades in relation to metal nanoparticle based SERS.<sup>10,12</sup> However, developing SERS substrates that have high enhancement and good signal reproducibility especially in the case of solution based metal nanoparticles involve the challenging task of orderly assembling the nanoparticles on solid platforms to have a consistent SERS effect.<sup>13</sup> This is because of the challenging task to orderly assemble the nanoparticles on solid platforms to have a consistent SERS effect. In addition, metallic nanoparticles are usually capped with stabilizing agent which may significantly interfere with the SERS spectrum of the target molecule.<sup>14</sup> Thus, researchers are always searching for a sensitive, stable, reproducible, easy to prepare and user friendly SERS platform in order to develop cost-effective SERS sensors that are suitable for practical in-field rapid detection by handheld Raman devices.

1  
2  
3  
4  
5  
6  
7  
8  
9  
10  
11  
12  
13  
14  
15  
16  
17  
18  
19  
20  
21  
22  
23  
24  
25  
26  
27  
28  
29  
30  
31  
32  
33  
34  
35  
36  
37  
38  
39  
40  
41  
42  
43  
44  
45  
46  
47  
48  
49  
50  
51  
52  
53  
54  
55  
56  
57  
58  
59  
60

In fact, close packing of metal nanoparticles within nanometer space is one of the vital requirements for an efficient SERS substrate that delivers enormous SERS enhancement. This is because the nano gaps between particles act as hot spots where an analyte molecule experiences strong magnetic field and subsequent Raman signal enhancement.<sup>15, 16</sup> The preparation of a highly sensitive SERS substrate by electrodeposition is one of the simple, cost effective and efficient approaches that can overcome many of the challenges and setbacks that are associated with the task of developing closely packed layer of noble metal nanoparticles on solid platform.<sup>3,</sup>  
<sup>17</sup> The advantage of an electrodeposition method is that the reduction of metal ions, and subsequent deposition of atoms to form particles, can be precisely controlled by fine tuning the applied potential and deposition time along with the right choice of electrolyte.<sup>3, 17</sup> Therefore critical parameters such as particle size, inter-particle distance and layer thickness can be precisely controlled by electrodeposition. Further, this method produces bare particles without any capping agent which eliminates potential interference from the capping agent Raman signature. In this work, we applied a simple and quick procedure for electrodeposition of closely packed single layer of gold nanostructures (AuNS) over a flat gold surface (pAu).<sup>17</sup> We preferred gold as the SERS amplifier since it is more stable than silver in open air environment. In addition, AuNS are good Raman photon enhancers under NIR excitation that is used in portable Raman devices.<sup>18</sup> Further, SERS substrate enhancement factor (SSEF) of the present pAu/AuNS surface has been precisely quantified by established renewed approach.<sup>17, 19</sup>

The explosive, 2,4,6-trinitrotoluene (TNT), is commonly used for industrial, military and recently in global terrorist activities.<sup>18</sup> Therefore, rapid in-field identification of TNT in soil and water is not only important to forensic and national security departments but also essential to improve the water and air quality. We recently demonstrated the synthesis of colored TNT:

1  
2  
3 cysteamine complex in aqueous media and its use for the detection of TNT by SERS.<sup>19</sup> We also  
4  
5 demonstrated that cysteamine in alkaline aqueous medium is not capable of forming a similar  
6  
7 complex with two important nitroaromatic compounds, 2, 4 dinitrotoluene (2,4-DNT) and picric  
8  
9 acid (PA), which are known to co-exist with TNT in environment.<sup>19, 20</sup> Both of these compounds  
10  
11 are also known to have Raman signatures that are similar to TNT. Therefore, the ability of  
12  
13 detecting TNT without interference from these compounds confirms the selectivity of the TNT:  
14  
15 cysteamine complex for the SERS detection of TNT.  
16  
17  
18  
19

20  
21 In our previous work, we used citrate capped gold nanoparticles as the SERS platform.<sup>21</sup>  
22  
23 The disadvantages of using gold nanoparticles were underlined by the high detection limit (1  
24  
25 nM) of TNT and limited reproducibility of the TNT SERS signals. These disadvantages are  
26  
27 attributed in part to the high polydispersity of the metallic nanoparticles as well as the use of a  
28  
29 drop-dry technique. In this technique the nanoparticles, after interaction with the TNT:  
30  
31 cysteamine complex, were dropped onto a metallic surface and dried. This led to  
32  
33 nonhomogeneous distribution of hotspots and hence the poor reproducibility of the SERS  
34  
35 spectra. Therefore, in this work we aim at using the new pAu/AuNS substrate in order to achieve  
36  
37 a proof of concept on the ultra-trace and reproducible detection of TNT in environment by  
38  
39 SERS. This proof of concept can be easily extended to the in-field SERS detection of many other  
40  
41 analytes by the pAu/AuNS substrate.  
42  
43  
44  
45  
46

## 47 **2. Experimental Section**

### 48 *2.1. Chemicals and Materials*

49  
50  
51  
52  
53 Hydrogen tetrachloroaurate (HAuCl<sub>4</sub>·4H<sub>2</sub>O), trisodium citrate, cysteamine hydrochloride,  
54  
55 sodium hydroxide, acetonitrile, ethanol and methanol were purchased from Sigma Aldrich  
56  
57 (USA). All chemicals and solvents were of analytical grade and were used without further  
58  
59  
60

1  
2  
3 purification. Synthesis of 1,8,15,22-tetraaminophthalocyanatocobalt(II) ( $4\alpha\text{-Co}^{\text{II}}\text{TAPc}$ ) was  
4 reported elsewhere.<sup>21</sup> 2,4,6-trinitrotoluene (TNT) standard (1 mg/ ml in 1:1 acetonitrile:  
5 methanol) was purchased from Merck (Australia). All dilutions were made using deionised water  
6 (18.2 M $\Omega$ .cm) from a Millipore water purification system. All other chemicals were of  
7 Analytical grade. The chemicals were used without any further purification. Polishing slurries  
8 and pads (Microcloth®) were purchased from Buehler, Germany. Polycrystalline gold discs (Au)  
9 having a geometric area of 0.502 cm<sup>2</sup> and platinum wire (A & E Metals, Australia) were  
10 respectively, used as working and counter electrode. Dry leakless electrode (DRIREF-2, World  
11 Precision Instruments, USA) was used as a reference electrode.  
12  
13  
14  
15  
16  
17  
18  
19  
20  
21  
22  
23  
24

## 25 2.2. Instrumentation

26  
27  
28 All electrochemical experiments were carried out in Autolab PGSTAT204 potentiostat  
29 with a custom-made three-electrode cell setup. All Raman measurements were performed using  
30 the Renishaw InVia Raman microscope equipped with 785 nm laser line as excitation source.  
31 Spectra were collected using a 50 $\times$  and 5x objective lens over a wavelength range from 500 cm<sup>-1</sup>  
32 to 2000 cm<sup>-1</sup> using a laser power of 1 mW for 10s (3 accumulations). For each TNT-cysteamine  
33 spectrum, 25 spectra were randomly recorded over the entire surface and averaged. SEM  
34 measurements were performed using Zeiss Sigma VP Field Emission Scanning Electron  
35 Microscope with an accelerating voltage of 5 kV under high vacuum.  
36  
37  
38  
39  
40  
41  
42  
43  
44  
45  
46  
47

## 48 2.3. SERS Substrate Preparation

49  
50 The synthesis of the pAu/AuNS substrate was carried out using our recently reported  
51 methodology with few modifications.<sup>17, 19</sup> Au disc electrodes were manually mirror-polished  
52 with alumina slurries of sequentially decreasing particle sizes (0.5  $\mu\text{m}$ , 0.05  $\mu\text{m}$  and 0.02  $\mu\text{m}$ ).  
53 After each step of polishing, the electrodes were immersed in Millipore water and subsequently  
54  
55  
56  
57  
58  
59  
60

1  
2  
3  
4  
5  
6  
7  
8  
9  
10  
11  
12  
13  
14  
15  
16  
17  
18  
19  
20  
21  
22  
23  
24  
25  
26  
27  
28  
29  
30  
31  
32  
33  
34  
35  
36  
37  
38  
39  
40  
41  
42  
43  
44  
45  
46  
47  
48  
49  
50  
51  
52  
53  
54  
55  
56  
57  
58  
59  
60

sonicated in an aqueous ultrasonic bath for 15 minutes in order to remove the physically adsorbed alumina particles from the electrode surface.

AuNS were developed over flat Au surface (pAu/AuNS) by potentiostatic deposition. Prior to the deposition of gold nanostructures, the Au discs were cleaned by immersing into piranha solution for 10 min (3:1, 98% H<sub>2</sub>SO<sub>4</sub> / 30% H<sub>2</sub>O<sub>2</sub>) and subsequent thorough washing with copious amount of Millipore water (warning: piranha solution is very corrosive and must be handled with extreme caution; it reacts violently with organic materials and should not be stored in tightly closed vessels). After cleaning the Au disc, a three-electrode electrochemical cell was filled with the solution of 4 mM H<sub>2</sub>AuCl<sub>4</sub> in 0.1 M HClO<sub>4</sub> and subsequently purged with high pure argon gas for 30 min to remove oxygen from solution. A potential of -80 mV was applied for 400 s and then the electrode was removed from the solution and subsequently washed with Millipore water to remove other ions from the surface. The electrode was then dried under a stream of nitrogen gas and used as a SERS substrate.

#### 2.4. Preparation of Meisenheimer complex with TNT

Cysteamine: TNT complex was prepared according to the recently developed procedure.<sup>19</sup> Briefly, cysteamine stock solution (2x 10<sup>-4</sup> M) was prepared in MilliQ water and the pH is adjusted to 8.5. Equal volumes of TNT and cysteamine having the desired concentration were mixed together. The mixture was then allowed to stand for 15 minutes until the pink color of the Meisenheimer complex is fully developed.

#### 2.5. Detection of TNT by SERS

After the preparation for the cysteamine-TNT complex at the desired concentration, 100µL aliquot of the complex was then dropped over the pAu/AuNS surface and allowed to



stand for 30 min in order to form a self-assembled monolayer of the TNT-cysteamine complex through the free thiol group of cysteamine. Subsequently, the substrate was thoroughly washed with copious amount of water to remove the unbounded and physically adsorbed TNT-cysteamine complex from the surface. The substrate was then dried in a stream of nitrogen gas and subsequently used for SERS measurement to identify the TNT. A laser source @785 nm was used in this work due to its availability. This NIR excitation wave length has been utilized in other SERS studied<sup>6, 21, 22</sup>.

### 2.6. Identification of TNT in soil

A known concentration of TNT was spiked into soil and subsequently extracted into water medium by washing the TNT treated soil with water and centrifugation. The extracted aqueous TNT was then interacted with cysteamine at pH 8.5 to form the Meisenheimer complex. Finally, the TNT-cysteamine complex was dropped onto pAu/AuNS substrate and allowed to stand for 30 min. The substrate was then washed with millipore water, dried and used for SERS measurements.

## 3. Results and Discussion

### 3.1. pAu/AuNS substrate preparation and characterization

The preparation of various nanostructures of gold via electrodeposition and its subsequent SERS application has been demonstrated in literatures.<sup>24, 25</sup> However, the majority of the reported substrates were non-homogenous and their surfaces lack highly ordered geometry. Therefore, in order to overcome these problems and to develop a homogenous surface, in the present work closely packed gold nanostructures were formed over Au surface. We optimized the electrodeposition conditions such as gold chloride concentration, applied potential,

1  
2  
3 deposition time and electrolyte. Figures S1 (A-C), shows the SEM of nanostructured gold  
4 substrates that are prepared at different applied potentials (-20 mV, -150 mV, and -300 mV). The  
5 figure clearly indicates the non-homogenous surfaces of the substrates. Figure 1 depicts the SEM  
6 of the nanostructured substrate, prepared at -400 mV, under different magnifications. It is clear  
7 for the figure that prepared at -400 mV has a more homogenous surface when compared to those  
8 of the other substrates prepared at -20 mV, -150mV, and -300 mV (S1 A-C).  
9  
10  
11  
12  
13  
14  
15  
16  
17

18 The close packing of single layer gold nanostructures within nanometer scale inter-  
19 particle distance is very critical for enormous SERS enhancement via hot spots and also for the  
20 reproducibility of the SERS signal over the entire surface.<sup>15, 16</sup> The SEM image of pAu/AuNS  
21 surface under wider magnification (Fig. 1A) reveals that the deposition of AuNS is almost  
22 uniform over the entire surface. Even under 100 micron magnification, the particle coverage was  
23 uniform and almost defect-free. We obtained consistent SEM pictures over the 8 mm diameter  
24 surface which clearly demonstrates that the electrodeposition method produced AuNS over the  
25 entire surface. The size of AuNS was in the range of 10-100 nm (Fig. 1C and D). Although the  
26 sizes of the AuNS are not highly monodisperse, till they are ideal for delivering homogeneous  
27 SERS signal when the spot diameter of the focused laser is micron scale as indicated by Fig. 2. A  
28 closer look at the magnified SEM image (Fig. 1C and D) reveals that the AuNS are deposited  
29 almost as a single layer. Further, the AuNS are closely packed having nanometer scale inter-  
30 particle space which led to creating vast number of hot spots. Therefore, despite the  
31 polydispersed particle size (10-100 nm), we believe that the homogeneity in particle coverage  
32 and inter-particle distance significantly reduces the variations of the SERS signal at different  
33 locations for a micron-scale diameter focused laser spot (*vide infra*).  
34  
35  
36  
37  
38  
39  
40  
41  
42  
43  
44  
45  
46  
47  
48  
49  
50  
51  
52  
53  
54  
55  
56  
57  
58  
59  
60

1  
2  
3  
4  
5  
6  
7  
8  
9  
10  
11  
12  
13  
14  
15  
16  
17  
18  
19  
20  
21  
22  
23  
24  
25  
26  
27  
28  
29  
30  
31  
32  
33  
34  
35  
36  
37  
38  
39  
40  
41  
42  
43  
44  
45  
46  
47  
48  
49  
50  
51  
52  
53  
54  
55  
56  
57  
58  
59  
60

At this juncture, it is worth focusing briefly on our choice of polished Au as the underlying platform. For the deposition of AuNS, choosing the same material (i.e., Au) as the underlying support allows several particle initiation spot which subsequently leads to smaller AuNS size and high packing density. In addition to the hot spot effect, a possible coupling between the propagating surface plasmon polariton (SPP) of the underlying polished Au surface and surface plasmon resonance (SPR) of the AuNS (i.e., SPP–SPR coupling)<sup>17, 26</sup> would lead to high SERS enhancement in comparison to the conventional SERS enhancement from nanoparticles only. In order to quantify the SERS substrate enhancement factor (SSEF), we applied a renewed electrochemical approach (see supplementary information)<sup>17, 19</sup>. The SSEF of pAu/AuNS surface has been precisely quantified and was found to be  $(2.2 \pm 0.17) \times 10^5$ .

The homogeneity of the substrate to deliver consistent SERS signal was demonstrated by randomly recording 150 surface-enhanced resonance Raman (SERRS) spectra of 4 $\alpha$ -Co<sup>II</sup>TAPc over the entire pAu/AuNS surface. The relative standard deviation (RSD) of 756 cm<sup>-1</sup> peak (Fig. 2A) was found to be 8.23% when a 50x objective is used to focus the laser beam (spot diameter = 0.64  $\mu\text{m}$ ; illuminated area = 0.32  $\mu\text{m}^2$ , see supplementary information). However, the RSD decreases down to 4.37% when a 5x objective is used where the diameter of the focused laser beam is around 3.99  $\mu\text{m}$  with a focusing area of 12.56  $\mu\text{m}^2$  (Fig. 2B). The observed decrease in RSD with increase in laser focusing area (5x objective has 39.25 times higher illumination area than 50x objective) is justified as the SERS signal becomes highly averaged with the increased focus of the objective. In our experiment, when using 5x objective, the SERS substrate is actually screened under wide area illumination (WAI) setting in comparison to 50x objective. This WAI setting allows for increased focusing area and, in effect, contributes to the enhanced reproducibility of the SERS signal.<sup>27, 28</sup> Thus, the obtained RSD of 4.37% for the laser beam

illumination area of  $12.56 \mu^2$  clearly confirms that the surface has high efficiency for reproducible SERS performance, especially under wide area illumination settings. The above results clearly indicate that the homogeneity in particle coverage, as a single layer, and the uniformity in particle packing density leads to with consistent hot spot distribution and homogeneous SERS signal.

### 3.2. SERS detection of TNT

Self-assembled monolayer of cysteamine-TNT Meisenheimer complex was formed over pAu/AuNS surface according to the experimental procedure. The advantage of the cysteamine-TNT Meisenheimer complex is that the cysteamine moiety of the complex is acting as a binding molecule that forms a strong Au-S bond with the nanostructured surface of the substrate<sup>21</sup>. Due to the very small length of the cysteamine molecule, the cyteamine- TNT complex is brought to a very short distance from the SERS substrate. Therefore, the Raman spectrum of TNT experiences a high enhancement by the SERS substrate. In addition cysteamine was proven by our group to selectively bind with TNT to form a Meisenheimer while other nitroaromatic compounds such as 2,4-DNt and picric acid did not form a similar complex at pH 8.5<sup>21</sup>. Fig. 3A (pink spectrum) depicts the SERS spectrum of the monolayer formed from 1 nM cysteamine-TNT complex. The SERS spectrum of cysteamine-TNT complex is dominated by C=C aromatic stretching vibration at  $1643 \text{ cm}^{-1}$  due to the vertical orientation of TNT over the pAu/AuNS surface and the large Raman cross-section of the aromatic ring.<sup>29-31</sup> The spectrum also depicted a sharp and intense band at  $1348 \text{ cm}^{-1}$  corresponding to  $\text{NO}_2$  group symmetric stretching vibration.<sup>29-31</sup> The other significant bands appearing at  $1292 \text{ cm}^{-1}$ ,  $1253 \text{ cm}^{-1}$  and  $797 \text{ cm}^{-1}$  corresponds to aromatic ring stretching,  $\text{C}_6\text{H}_2\text{-C}$  vibration and C-H out of plane bending, respectively.<sup>29-31</sup> The SERS spectrum of cysteamine monolayer alone does not show any

1  
2  
3 significant Raman bands at a concentration of 10 pM. However, it showed significant Raman  
4  
5 bands for monolayer formed at higher concentration ( $10^{-5}$  M) which is depicted in Fig. S2.  
6  
7

8  
9 In order to demonstrate the suitability of the present Au/AuNS towards SERS  
10  
11 quantification, various concentrations of cysteamine-TNT complex were prepared and  
12  
13 monolayer modified Au/AuNS substrates were screened under the Raman microscope. Fig. 3A  
14  
15 shows the SERS spectrum of the cysteamine-TNT monolayer within a concentration range of 1  
16  
17 nM-100 fM (the spectra were normalized and background subtracted). For each concentration,  
18  
19 25 spectra were randomly recorded over the entire surface and averaged. The band centered at  
20  
21 1348  $\text{cm}^{-1}$  corresponding to  $\text{NO}_2$  symmetric stretching of TNT was used as a reference band for  
22  
23 TNT quantification. The SERS signals were found to be monotonically decreasing with the  
24  
25 decreased concentration (Fig. S3) while the spectral features remain identical for each  
26  
27 concentration. Even at the concentration of 100 fM, the spectral features of TNT can still be  
28  
29 observed (Fig. 3A inset). The linear relation between SERS signal intensity at 1348  $\text{cm}^{-1}$  and the  
30  
31 corresponding log concentration of cysteamine:TNT complex is depicted in Fig. 3B. The linear  
32  
33 relationship between log (concentration) and SERS intensity was previously demonstrated in the  
34  
35 literature<sup>33,34</sup>. As indicated by the Fig. 3B, good correlation ( $R^2 = 0.992$ ) was found over a wide  
36  
37 concentration range of TNT ( $10^{-9}$ -  $10^{-13}$  M)  
38  
39  
40  
41  
42  
43  
44

45 The SERS spectrum of the cysteamine:TNT complex showed good Raman counts  
46  
47 (around 1000 counts as an average) even for a very low concentration of 100 fM (Fig. 3A inset).  
48  
49 This clearly demonstrates that pAu/AuNS surface is highly sensitive which is credited to the  
50  
51 close packing of AuNS with nanometer scale inter-particle distance generating several hotspots.  
52  
53 The shorter chain length (2 carbons) of cysteamine may also be responsible for the higher SERS  
54  
55 signal of TNT since the SERS signal decreases by a factor of  $10^{-12}$  while increasing the distance  
56  
57  
58  
59  
60

1  
2  
3 between the analyte and Raman enhancing surface.<sup>35</sup> At the low concentration of 100 fM, the  
4  
5 observed SERS spectra would be reported from single hot spots. Thus, SERS temporal changes  
6  
7 using 50x objective may show blinking and, hence, the ultra-high sensitivity of the SERS  
8  
9 substrate<sup>36</sup>.  
10

### 11 12 13 14 *3.3. Identification of TNT in soil*

15  
16 Finally, the practical application of pAu/AuNS substrate has been demonstrated by  
17  
18 identifying TNT in soil sample (see experimental section). Prior to spiking the soil matrix with  
19  
20 TNT solution, the sample has been tested for any pre-existing TNT within the matrix and the  
21  
22 SERS spectrum of the extract confirms the absence of any such pre-existing TNT. Conversely,  
23  
24 after spiking the TNT into the soil matrix and subsequent extracted TNT-cysteamine complex  
25  
26 (Fig. 4; red spectrum) showed almost identical Raman fingerprints to that of fresh TNT-  
27  
28 cysteamine complex. This clearly demonstrates that the present methodology can be employed to  
29  
30 identify TNT in-field for environmental and forensic applications.  
31  
32  
33  
34  
35

## 36 **4. Conclusion**

37  
38 In conclusion, the present study has simultaneously demonstrated the strength of  
39  
40 electrodeposition method and SERS technique by producing an ultra-sensitive SERS substrate  
41  
42 and identifying 100 fM of TNT, respectively. By identifying 1 nM of TNT in soil we have  
43  
44 demonstrated a proof of concept for the rapid in-field identification of ultra-trace amounts of  
45  
46 TNT by using a small molecule to selectively bind to the analyte and immobilize it onto our  
47  
48 ultrasensitive SERS substrate. Presently, we are involved in developing disposable SERS strips  
49  
50 based on the present electrochemical approach to be coupled with portable Raman device as a  
51  
52 readout approach for in-field analysis.  
53  
54  
55  
56  
57  
58  
59  
60

## 5. Acknowledgement

The Authors sincerely thank Dr. Llew Rintoul from QUT for his valuable discussion and support.

## References

1. S.-C. Luo, K. Sivashanmugan, J.-D. Liao, C.-K. Yao and H.-C. Peng, *Biosensors and Bioelectronics*, 2014, 61, 232-240.
2. X. X. Han, L. Chen, U. Kuhlmann, C. Schulz, I. M. Weidinger and P. Hildebrandt, *Angewandte Chemie - International Edition*, 2014, 53, 2481-2484.
3. A. Sivanesan, E. Witkowska, W. Adamkiewicz, Ł. Dziewit, A. Kamińska and J. Waluk, *Analyst*, 2014, 139, 1037-1043.
4. G. Kalaivani, N. S. V. Narayanan, A. Sivanesan, A. Kannan, A. Kaminska and R. Sevel, *RSC Advances*, 2013, 3, 6839-6846.
5. G. Kalaivani, A. Sivanesan, A. Kannan, N. S. Venkata Narayanan, A. Kaminska and R. Sevel, *Langmuir*, 2012, 28, 14357-14363.
6. J. Hughes, E. L. Izake, W. B. Lott, G. A. Ayoko and M. Sillence, *Talanta*, 2014, 130, 20-25.
7. C. L. Haynes, A. D. McFarland and R. P. Van Duyne, *Analytical Chemistry*, 2005, 77, 338 A-346 A.
8. K. Kneipp, H. Kneipp, I. Itzkan, R. R. Dasari and M. S. Feld, *Journal of Physics Condensed Matter*, 2002, 14, R597-R624.
9. Y. S. Yamamoto, Y. Ozakic and T. Itoh, *Journal of Photochemistry and Photobiology C: Photochemistry Reviews*, 2008, 21, 81-104
10. J. N. Anker, W. P. Hall, O. Lyandres, N. C. Shah, J. Zhao and R. P. Van Duyne, *Nature Materials*, 2008, 7, 442-453.
11. S. Nie and S. R. Emory, *science*, 1997, 275, 1102-1106.
12. P. L. Stiles, J. A. Dieringer, N. C. Shah and R. P. Van Duyne, in *Annual Review of Analytical Chemistry*, 2008, vol. 1, pp. 601-626.
13. Y.S. Yamamoto, K. Hasegaw, Y. Hasegaw, N.Takahashi, Y. Kitaham, S. Fukuok, N. Murase, Y. Baba, Y. Ozakid and T. Itoh, *Physical Chemistry Chemical Physics*, 2015, 13, 14611-14615.
14. J. Jiang, L. Ou-Yang, L. Zhu, J. Zou and H. Tang, *Sci. Rep.*, 2014, 4.
15. A. W. Clark and J. M. Cooper, *Small*, 2011, 7, 119-125.
16. M. Yang, R. Alvarez-Puebla, H. S. Kim, P. Aldeanueva-Potel, L. M. Liz-Marzán and N. A. Kotov, *Nano Letters*, 2010, 10, 4013-4019.
17. A. Sivanesan, W. Adamkiewicz, G. Kalaivani, A. Kaminska, J. Waluk, R. Holyst and E. L. Izake, *Analyst*, 2015, 140, 489-496.
18. H. Chu, J. Wang, L. Ding, D. Yuan, Y. Zhang, J. Liu and Y. Li, *Journal of the American Chemical Society*, 2009, 131, 14310-14316.
19. A. Sivanesan, W. Adamkiewicz, G. Kalaivani, A. Kamińska, J. Waluk, R. Hołyst and E. L. Izake, *Electrochemistry Communications*, 2014, 49, 103-106.
20. E. R. Goldman, I. L. Medintz, J. L. Whitley, A. Hayhurst, A. R. Clapp, H. T. Uyeda, J. R. Deschamps, M. E. Lassman and H. Mattoussi, *Journal of the American Chemical Society*, 2005, 127, 6744-6751.
21. A. K. Jamil, E. L. Izake, A. Sivanesan and P. M. Fredericks, *Talanta*, 2015, 134, 732-738.
22. Y. Jiang, H. Zhao, N. Zhu, Y. Lin, P. Yu and L. Mao, *Angewandte Chemie - International Edition*, 2008, 47, 8601-8604.
23. A. Sivanesan and S. Abraham John, *Langmuir*, 2008, 24, 2186-2190.



- 1
  - 2
  - 3
  - 4
  - 5
  - 6
  - 7
  - 8
  - 9
  - 10
  - 11
  - 12
  - 13
  - 14
  - 15
  - 16
  - 17
  - 18
  - 19
  - 20
  - 21
  - 22
  - 23
  - 24
  - 25
  - 26
  - 27
  - 28
  - 29
  - 30
  - 31
  - 32
  - 33
  - 34
  - 35
  - 36
  - 37
  - 38
  - 39
  - 40
  - 41
  - 42
  - 43
  - 44
  - 45
  - 46
  - 47
  - 48
  - 49
  - 50
  - 51
  - 52
  - 53
  - 54
  - 55
  - 56
  - 57
  - 58
  - 59
  - 60
24. S. Choi, M. Ahn and J. Kim, *Analytica Chimica Acta*, 2013, 779, 1-7.
25. Z. Y. Lv, L. P. Mei, W. Y. Chen, J. J. Feng, J. Y. Chen and A. J. Wang, *Sensors and Actuators, B: Chemical*, 2014, 201, 92-99.
26. N. Félidj, J. Aubard, G. Lévi, J. R. Krenn, G. Schider, A. Leitner and F. R. Aussenegg, *Physical Review B*, 2002, 66, 245407.
27. K. Shin and H. Chung, *Analyst*, 2013, 138, 3335-3346.
28. K. Shin, K. Ryu, H. Lee, K. Kim, H. Chung and D. Sohn, *Analyst*, 2013, 138, 932-938.
29. X. He, H. Wang, Z. Li, D. Chen and Q. Zhang, *Physical Chemistry Chemical Physics*, 2014, 16, 14706-14712.
30. S. Sil, D. Chaturvedi, K. B. Krishnappa, S. Kumar, S. N. Asthana and S. Umapathy, *The Journal of Physical Chemistry A*, 2014, 118, 2904-2914.
31. R. Kanchanapally, S. S. Sinha, Z. Fan, M. Dubey, E. Zakar and P. C. Ray, *The Journal of Physical Chemistry C*, 2014, 118, 7070-7075.
32. S. S. R. Dasary, A. K. Singh, D. Senapati, H. Yu and P. C. Ray, *Journal of the American Chemical Society*, 2009, 131, 13806-13812.
33. Z. Guo, J. Hwang, B. Zhao, J. H. Chung, S. G. Cho, S. Baekd, J. Choo, *Analyst*, 2014, 139, 807-812.
34. M. Liu, W. Chen, *Biosensors and Bioelectronics*, 2013, 46, 68-73.
35. A. Sivanesan, J. Kozuch, H. K. Ly, G. Kalaivani, A. Fischer and I. M. Weidinger, *RSC Advances*, 2012, 2, 805-808.
36. R. Botta, G. Upender, R. Sathyavathi, D. N. Rao, C. Bansal, *Materials Chemistry and Physics*, 2013, 137, 699-703.

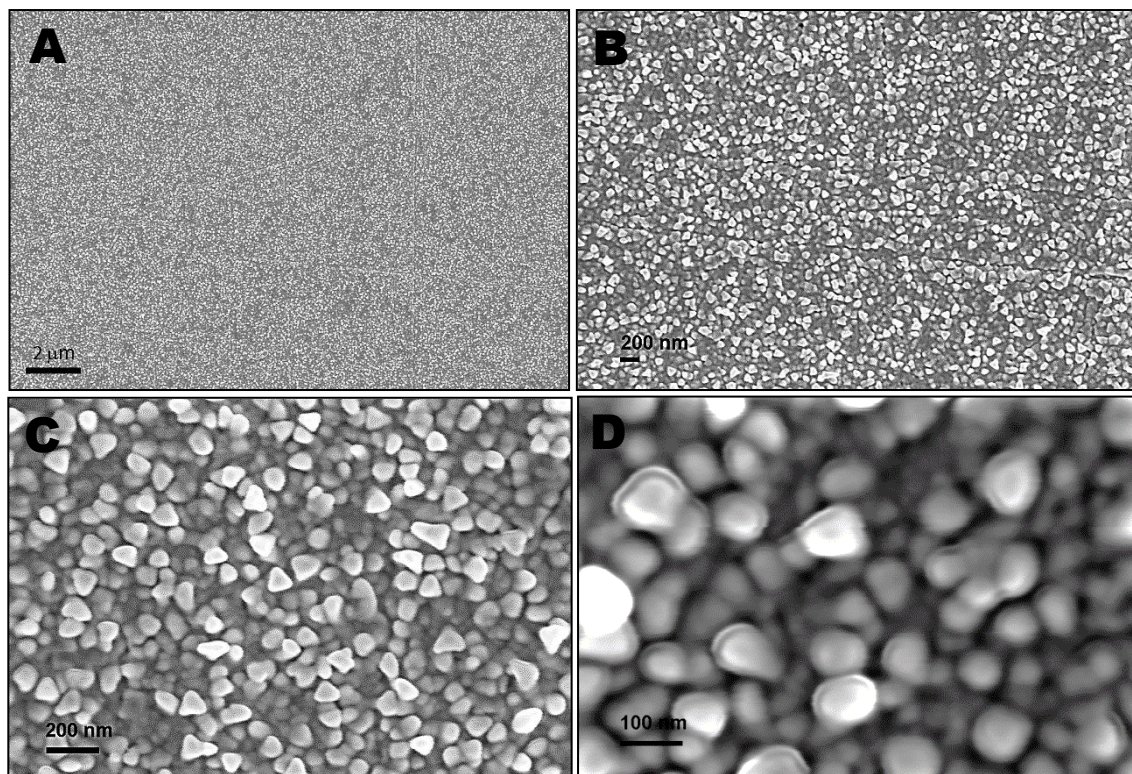


**Fig. 1** (A-D) SEM images of pAu/AuNS surface under different magnifications.

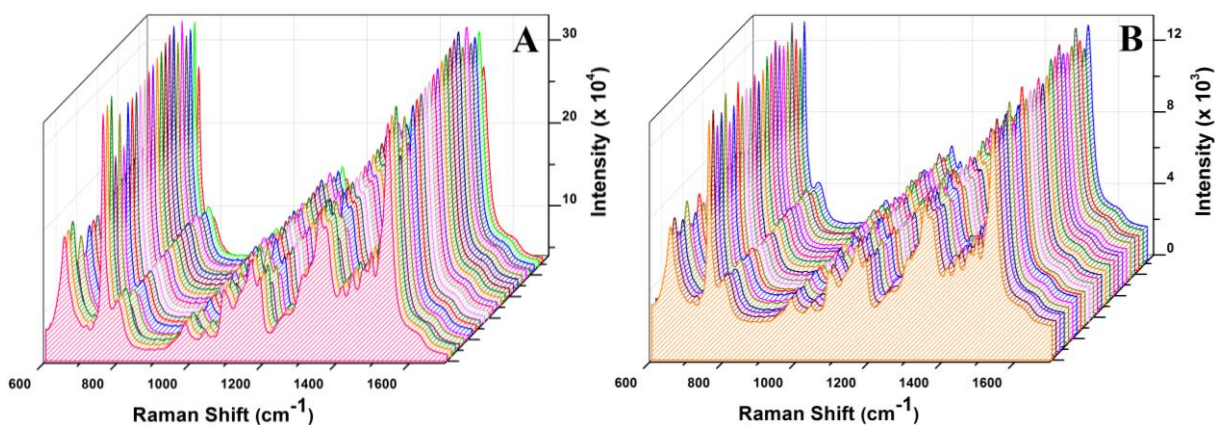


**Fig. 2** A series of SERRS spectra of 4 $\alpha$ -Co<sup>II</sup>TAPc randomly collected over the entire 8 mm diameter pAu/AuNS disc using (A) 50x objective with a laser focusing area of 0.32  $\mu^2$  and (B) 5x objective with a laser focusing area of 12.56  $\mu^2$ .

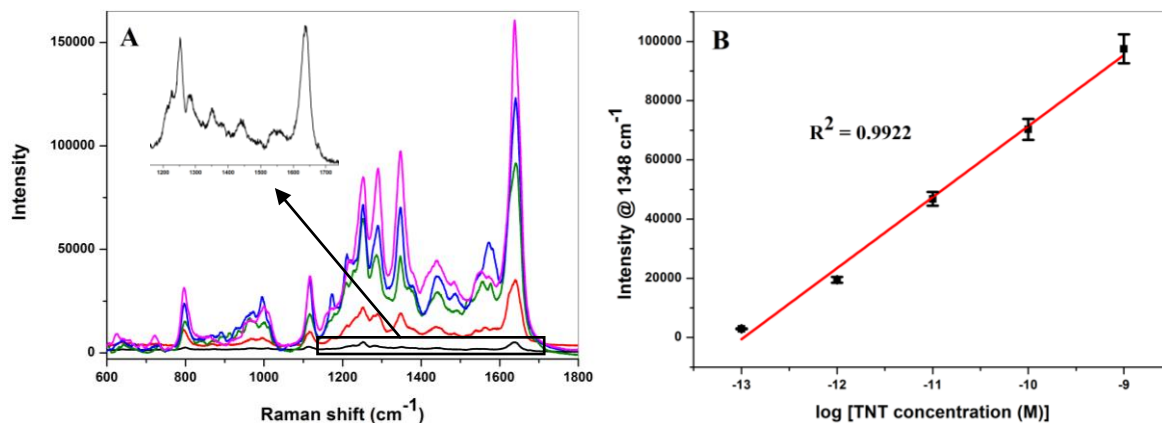


**Fig. 3** (A) SERS spectra of decreasing TNT concentration: 1 nM (*pink*), 100 pM (*blue*), 10 pM (*green*), 1 pM (*red*), 100 fM (*black*). Inset shows a closer view of 100 fM spectrum. For each concentration, 25 spectra were randomly recorded over the entire surface and averaged. (B) Plot demonstrating the linear relation between log the concentration of TNT and Raman intensity @1348 cm<sup>-1</sup>.

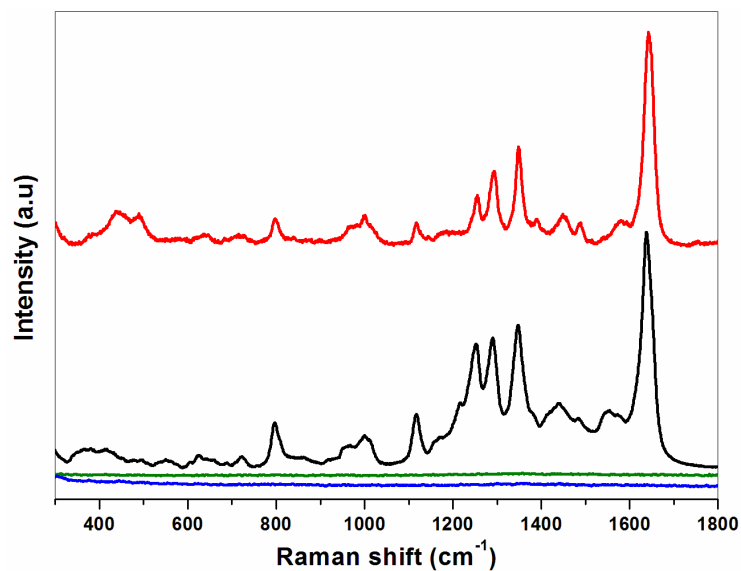


**Fig. 4** Monolayer SERS spectra of bare pAu/AuNS (*blue*), 10 pM cysteamine (*green*), 1 nM - cysteamine-TNT (*black*) and 1 nM soil extracted TNT complexed with cysteamine (*red*) on pAu/AuNS surfaces.